DOI: 10.1002/ejic.200800167

Study of the Effect of the Phosphane Bridging Chain Nature on the Structural and Photophysical Properties of a Series of Gold(I) Ethynylpyridine Complexes

Montserrat Ferrer,*[a] Albert Gutiérrez,[a] Laura Rodríguez,[a,b] Oriol Rossell,[a] João C. Lima,[b] Mercè Font-Bardia,[c] and Xavier Solans[c]

Keywords: Gold / Aurophilicity / Phosphanes / Alkynes / Luminescence / UV/Vis spectroscopy

Alkynyl Au^I complexes of the type $[Au(C{\equiv}CC_5H_4N)(PPh_3)]$ (**1**) $[Au_2(C{\equiv}CC_5H_4N)_2$ (diphosphane)] [diphosphane = bis(diphenylphosphanyl)methane (**2**), bis(diphenylphosphanyl)isopropane] (**3**), bis(diphenylphosphanyl)acetylene (**4**), 1,2-bis(diphenylphosphanyl)ethane (**5**), 1,3-bis(diphenylphosphanyl)propane (**6**), 1,4-bis(diphenylphosphanyl)butane (**7**), 1,1′-bis(diphenylphosphanyl)ferrocene (**8**) and $[Au_3(C{\equiv}C\text{-}C_5H_4N)_3$(triphos)] [triphos = 1,1,1-tris(diphenylphosphanylmethyl)ethane] (**9**) were prepared by reaction of $[Au(C{\equiv}CC_5H_4N)]_n$ with the suitable phosphane. Determination of the X-ray crystal structures of several compounds bearing different carbon backbones between the phosphorus atoms reveals the influence of the nature of the phosphane spacer on the establishment of intra and/or intermolecular gold–gold interactions. The absorption and emission properties of the complexes were analysed by taking into account the presence or absence of intermetallic interactions. Although UV/Vis spectra show differences for compounds with intramolecular Au–Au contacts, a conclusive trend was not observed in the emission behaviour.

Introduction

During the past years, there has been a continued interest in the chemistry of alkynyl gold(I) complexes, primary resulting from their interesting physical properties such as nonlinear optical behaviour,[1–3] liquid-crystalline properties[4,5] and photoemissive properties of the molecules and their aggregates.[6–12] Moreover, the low steric congestion about the linear gold(I) centre and the ability of gold(I) to form attractive Au···Au interactions have made alkynyl gold(I) compounds attractive candidates for the synthesis of a wide variety of supramolecular structures[13] as polymers,[14–17] macrocycles[18–20] or catenanes.[21–24]

One rather unexplored way of building up metallamacrocycles containing these subunits is to utilise alkynyl ligands with a second binding site. In this context, the introduction of ethynylpyridine fragments into alkynyl gold(I) complexes allows the obtention of potentially useful building blocks towards the synthesis of heterometallic macrocycles or polymers. Although monophosphane compounds $[Au(C{\equiv}CC_5H_4N)$(phosphane)] have been recently reported (phosphane = PPh_3,[25] PCy_3[26]), there is no previous reports on the parent polyphosphane complexes, which is rather surprising in view of the tempting possibilities these gold(I) derivatives offer. Even more, the incorporation of gold(I) alkyne fragments into supramolecular architectures containing cavities can confer upon them emissive properties that could allow their utilisation as sensors in molecular recognition processes.

In this work, several polyphosphane ligands were used to prepare di- and trialkynyl gold(I) derivatives as an extension of our studies on the synthesis of suitable gold(I) alkynyls[27] to be used as polytopic metalloligands in self-assembly reactions. The alkynyl ligand was kept constant while the length and/or nature of the bridging carbon chain of the phosphane were varied to assess their effect on the existence of intra- or intermolecular Au···Au interactions. Moreover, a systematic analysis of their electronic absorption and emission properties was undertaken in order to show how the observed profiles would relate to the existence of aurophilic interactions.

Results and Discussion

Following a literature procedure,[28] the reaction of a dichloromethane suspension of $[Au(C{\equiv}CC_5H_4N)]_n$ with either PPh_3 (1 equiv.), dppm [bis(diphenylphosphanyl)-methane], dppip [bis(diphenylphosphanyl)isopropane], dppa [bis(diphenylphosphanyl)acetylene], dppe [1,2-bis(diphenylphosphanyl)ethane], dppp [1,3-bis(diphenylphosphanyl)propane], dppb [1,4-bis(diphenylphosphanyl)bu-

[a] Departament de Química Inorgànica, Universitat de Barcelona, c/ Martí i Franquès 1-11, 08028 Barcelona, Spain
Fax: +34-93-490-7725
E-mail: montse.ferrer@qi.ub.es
[b] REQUIMTE, Departamento de Química. Centro de Química Fina e Biotecnologia, Universidade Nova de Lisboa, Quinta da Torre, 2825 Monte de Caparica, Portugal
[c] Departament de Cristal·lografia, Mineralogia i Dipòsits Minerals, Universitat de Barcelona, c/ Martí i Franquès s/n, 08028 Barcelona, Spain
Supporting information for this article is available on the WWW under http://www.eurjic.org or from the author.

tane] and dppf [1,1′-bis(diphenylphosphanyl)ferrocene] (0.5 equiv.) or triphos [1,1,1-tris(diphenylphosphanylmethyl)ethane] (0.3 equiv.) afforded the desired complexes $[Au(C{\equiv}CC_5H_4N)(PPh_3)]$ (**1**), $[Au_2(C{\equiv}CC_5H_4N)_2(\mu_2\text{-diphosphane})]$ (**2**–**8**) or $[Au_3(C{\equiv}CC_5H_4N)_3(\mu_3\text{-triphos})]$ (**9**) in a yields greater than 60% (Scheme 1). Subsequent recrystallisation from dichloromethane/petroleum ether or dichloromethane/diethyl ether mixtures gave colourless-to-yellow crystals of **1**–**9**. All the synthesised compounds gave satisfactory elemental analysis and were characterised by ^1H, ^{31}P and ^{13}C NMR spectroscopy, mass spectrometry (ESI+) and IR spectroscopy. The structures of complexes **3**–**7** and **9** were determined by X-ray crystallography.

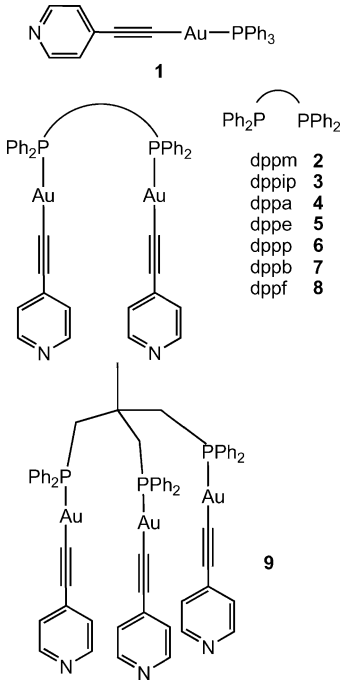

Scheme 1.

The IR spectra of all the complexes show weak absorption bands at 2103–2120 cm^{-1}, which is typical for the ν(C≡C) stretch of the alkynyl unit. The MS (ESI+) spectra show the peak due to the mono- $[M + H]^+$ (**1**), di- $[M + 2H]^{2+}$ (**2**–**8**) or triprotonated $[M + 3H]^{3+}$ (**9**) species as the most intense signals.

The NMR spectra of the complexes are consistent with the proposed structures. The ^1H NMR spectra show the expected signals for the α and β protons of the pyridine rings as well as those attributable to the phosphane ligands. The ^{31}P NMR spectra display a single resonance, which is shifted downfield (ca. 50 ppm) from that of the corresponding free phosphanes. The ^{13}C NMR spectra reveal the presence of the acetylenic carbon atoms bonded to gold, as two sets of resonances, whose assignments are based on gHMBC and gHSQC experiments, can be found at ca. 140 (Au–*C*≡C) and 100 (Au–C≡*C*) ppm. In most of the compounds, these signals exhibit coupling to the neighbouring ^{31}P atoms ($J \approx 140$ Hz and $J \approx 20$ Hz for Au–*C*≡C and Au–C≡*C*, respectively), appearing either as doublets (dppp, dppb, dppf and triphos compounds) or as AXX′ (A = ^{13}C; X = X′ = ^{31}P) spin systems (dppm and dppip compounds) (Figure 1). These chemical shifts and coupling constants are consistent with other reported molecules containing P–Au–C≡C units.[17,26,29] In addition, the phenyl rings of dppm and dppip show multiplets or apparent triplets for their *ortho*-, *meta*- and *ipso*-C atoms. The occurrence of second-order effects in this kind of compounds was attributed to a large ^{31}P-^{31}P coupling constant and/or to the existence of intramolecular gold–gold interactions in solution.[30]

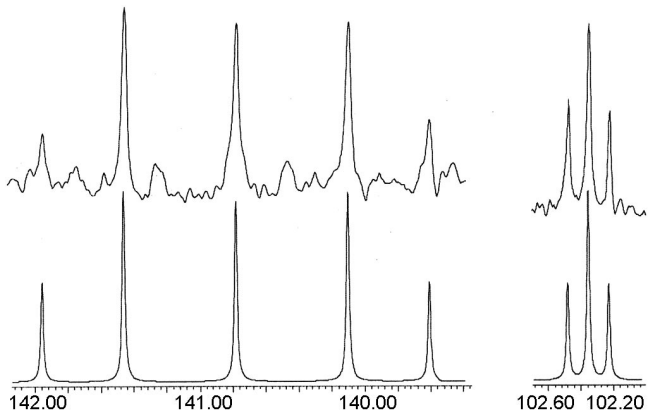

Figure 1. Expansions of ^{13}C NMR signals corresponding to the P–Au–*C*≡C (left) and P–Au–C≡*C* (right) fragments for dppip compound **3**.Top: experimental, bottom: simulations of the A part of AXX′ spin system.

In sharp contrast with the other phosphanes, when the gold polymer $[Au(C{\equiv}CC_5H_4N)]_n$ was treated with dppbz [1,2-bis(diphenylphosphanyl)benzene] in a molar ratio ≥1:1, under the same conditions as those reported above, the ionic compound $[Au(dppbz)_2][Au(C{\equiv}CC_5H_4N)_2]$ (**10**) was obtained (Scheme 2). Although the cationic part contains a bis(chelated) tetrahedral gold atom, the anion is a linear bis(alkynyl)gold compound recently described by us.[27] ^1H NMR and ^{13}C NMR spectra together with MS (ESI) spectra, which display the peaks corresponding to the $[Au(dppbz)_2]^+$ cation (*m*/*z* = 1089.2) and the $[Au(C{\equiv}CC_5H_4N)_2]^-$ anion (*m*/*z* = 401.3), constitute clear evidence of the nature of compound **10**. This anomalous behaviour was already observed for the analogous dppm ligand, which gave the trinuclear complex $[Au_3(dppm)_2(C{\equiv}CC_6H_5)_2][Au(C{\equiv}CC_6H_5)_2]$[31] instead of the expected

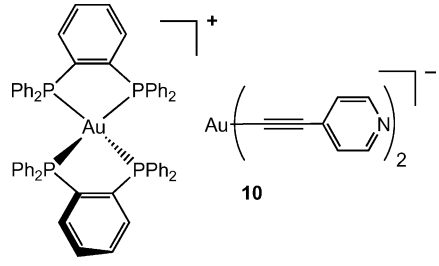

Scheme 2.

dinuclear compound $[Au_2(C{\equiv}CC_6H_5)_2(\mu^2\text{-dppm})]$ when it was allowed to react with the gold polymer $[Au(C{\equiv}CC_6H_5)]_n$.

X-ray Crystal Structures

In order to explore whether the nature of the carbon chain of the phosphane can influence the existence of intra and/or intermolecular aurophilic interactions in the solid state, a systematic study of the crystal structures of a series of compounds bearing phosphanes with different backbones was undertaken. Selected bond lengths and angles are listed in Tables 1–6.

The unit cell of dppip derivative **3** (one sp^3 carbon atom between the phosphorus atoms of the diphosphane) shows two independent but closely similar molecules that display intramolecular Au···Au contacts of 3.237(2) and 3.235(2) Å (only one molecule is shown in Figure 2). These distances (Table 1) are longer than that reported for the related $[Au_2(\mu_2\text{-dppip})_2]^{2+}$ [2.9275(10) Å],[32] $[Au_2(C{\equiv}CC_6H_5)_2\{\mu_2\text{-}Ph_2PN(n\text{Pr})PPh_2\}]$ [2.8404(8) Å],[9] $[Au_2(C{\equiv}CC_6H_4Me)_2\{\mu_2\text{-}Ph_2PN(n\text{Pr})PPh_2\}]$ [3.0708(7) Å],[9] $[Au_2(C_{14}H_9)_2(\mu_2\text{-dppm})]$ [3.0121(7) Å],[33] $[Au_2\{S_2P(p\text{-}C_6H_4OCH_3)(OC_5H_9)\}_2(\mu_2\text{-dppm})]$ [3.0353(3) Å],[34] $[Au_2(C_6H_5)_2(\mu_2\text{-dppm})]$ [3.154(1) Å][35] and $[Au_2(C_6F_5)_2(\mu_2\text{-dppm})]$ [3.163(1) Å][36] complexes, but shorter than that found for $[Au_2(C{\equiv}CC_6H_5)_2(\mu_2\text{-dppm})]$ [3.331(1) Å][37] or $[Au_2(CH_3)_2(\mu_2\text{-dppm})]$ [3.251(1) Å].[35] The observed torsion angles for Au–P–P′–Au (7.81 and 6.55°) are indicative of a parallel arrangement of the $Au(C{\equiv}CC_5H_4N)$ units, which are the dihedral angles between the two terminal pyridine rings 63.5(7) and 50.4(6)°. As it can be seen in Figure 2, one of the arms of the molecule displays a significant deviation from linearity, P–Au–C [170.6(3) and 169.2(3)] and Au–C–C [163.5(9) and 169.3(9)], probably as a result of packing forces.

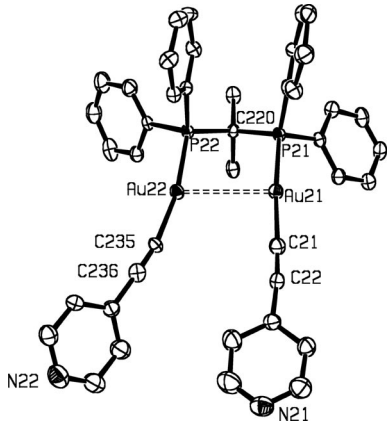

Figure 2. Molecular structure of $[Au_2(C{\equiv}CC_5H_4N)_2(\mu_2\text{-dppip})]$ (**3**).

The dppa compound (**4**) (two sp carbon atoms between the phosphorus atoms) is shown in Figure 3 and its data is gathered in Table 2. This complex crystallises as a dimer with inversion symmetry, which has two gold–gold interactions [2.9789(15) Å]. The value for the Au···Au contact is the shortest reported for this kind of diphosphanyl compounds: $[Au_2Cl_2(\mu_2\text{-dppe})]$ [3.187(1) Å],[38] $[Au_2Cl_2(\mu_2\text{-dpma})]$ [dpma = bis(diphenylphosphanyl)methylphenylarsine] [3.141(1) Å],[39] $[Au_2(C{\equiv}CC_6H_5)_2(\mu_2\text{-dppe})]$ [3.153(2) Å],[40] $[Au_2(CN)_2(\mu_2\text{-dppe})]$ (3.176 Å),[41] $[Au_2Cl_2(\mu_2\text{-ptp})]$ (ptp = 2,5-diphenylphosphanylthiophene) [3.0966(5) Å],[42] $[Au_2(4\text{-}SC_5H_4N)_2(\mu_2\text{-}Ph_2PCH{=}CHPPh_2)]$ (3.239 Å)[43] and $[Au_4(CNC)(\mu_2\text{-dppa})]$ (CNC = pyridyl-2,2-diphenyl) [3.189(2) Å].[44] In this case, the observed torsion angle for Au–P–P′–Au is 72.48°, which allows the formation of a 12-membered metallamacrocycle with each of the Au–Au bonds lying below and above the plane defined by the phosphorus atoms of the diphosphane. In addition, the extended structure of **4** presents secondary C–H···π(ring) interactions between different dimeric units that arise from the C–H bonds of pyridine groups and the nearest aromatic rings of either a diphosphane or a pyridine ligand.

Table 1. Selected bond lengths [Å] and angles [°] of **3**.

Au21···Au22	3.235(2)	P21–Au21–C21	174.1(3)
Au21–P21	2.284(3)	Au21–C21–C22	175.2(9)
Au21–C21	2.007(10)	P22–Au22–C235	169.2(3)
Au22–P22	2.280(3)	Au22–C235–C236	169.3(9)
Au22–C235	2.039(8)	C21–Au21···Au22	92.2(3)
C21–C22	1.195(12)	P21–Au21···Au22	91.63(8)
C235–C236	1.147(12)	C235–Au22···Au21	107.3(2)
		P22–Au22···Au21	83.45(7)
		P21–C220–P22	109.2(4)

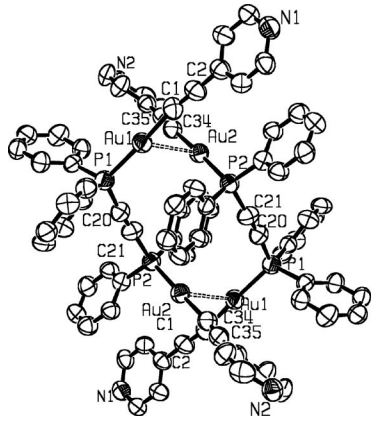

Figure 3. Molecular structure of $[Au_2(C{\equiv}CC_5H_4N)_2(\mu_2\text{-dppa})]$(**4**).

Table 2. Selected bond lengths [Å] and angles [°] of **4**.

Au1···Au2	2.9789(15)	P1–Au1–C1	173.7(3)
Au1–P1	2.271(3)	Au1–C1–C2	170.5(9)
Au1–C1	1.990(9)	P2–Au2–C34	175.9(2)
Au2–P2	2.281(2)	Au2–C34–C35	171.4(8)
Au2–C34	2.083(8)	C1–Au1···Au2	79.6(3)
C1–C2	1.251(12)	P1–Au1···Au2	106.46(7)
C34–C35	1.108(12)	C34–Au2···Au1	85.7(2)
C20–C21	1.149(12)	P2–Au2···Au1	96.45(7)
		C20–C21–P2	175.8(9)

The structures of the dppe (**5**), dppp (**6**) and dppb (**7**) derivatives (two, three and four methylene groups between the phosphorus atoms, respectively) (Figure 4, Table 3; Figure 5, Table 4; Figure 6, Table 5 and Figure 7, Table 6) are centrosymmetric. Both **5** and **7** display linear P–Au–C≡C–

units lying on the molecular plane with opposite orientation and a Au1–P1–P1a–Au1a torsion angle of 180° (diphosphane ligand in the *anti* conformation). Many examples of crystal structures for related dppe or dppb digold compounds can be found in the literature. Although in the majority of them an *anti* conformation for both ligands is observed, the association between the different molecules by the establishment of intermolecular aurophilic interactions can led to the formation of either polymeric chains[43,45–48] or independently packed molecules.[34,43,49,50] In our case, the establishment of gold–gold contacts [3.215(2) Å] between adjacent molecules for compound **5** led to the formation of a one-dimensional extended chain (Figure 5). There are no additional interactions between the different polymeric chains. In contrast, the crystal structure of dppb derivative **7** (Figure 6) shows the packing of simple molecular entities with no gold–gold interactions. In this latter case, crystallisation solvents could play an important role for the lack of aurophilic contacts.[51]

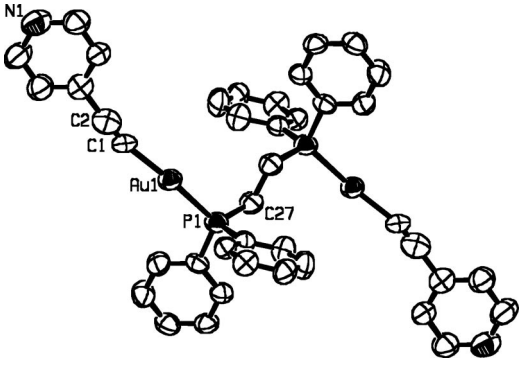

Figure 4. Molecular structure of $[Au_2(C{\equiv}CC_5H_4N)_2(\mu_2\text{-dppe})]$(**5**).

Table 3. Selected bond lengths [Å] and angles [°] of **5**.

Au1–P1	2.272(3)	P1–Au1–C1	175.2(3)
Au1–C1	2.064(11)	Au1–C1–C2	167.5(12)
C1–C2	1.009(14)	Au1–P1–C27	114.7(3)

A different situation is found in dppp compound **6** (Figure 7), in which the diphosphane adopts a less-twisted conformation [torsion angle Au1–P1–P1a–Au1a equal to 84.44°]. This is a common trend for dppp compounds, as a CDS search for related compounds (10 structures) shows the value of the torsion angles to be in the range from 51° in $[Au_2(\text{purin-6-ylamine-9-ate})_2(\mu_2\text{-dppp})]$[48] to 149.08° in $[Au_2(SC_6H_5)_2(\mu_2\text{-dppp})]$;[43] this fact is in contrast with the tendency of both dppe and dppb compounds to adopt torsional angles of 180°. The packing diagram shows no close aurophilic intermolecular interactions.

Table 4. Selected bond lengths [Å] and angles [°] of **6**.

Au–P	2.2790(16)	P–Au–C1	175.57(17)
Au–C1	1.985(6)	Au–C1–C2	174.3(6)
C1–C2	1.212(8)	Au–P–C20	115.50(18)
		P–C20–C21	116.8(3)

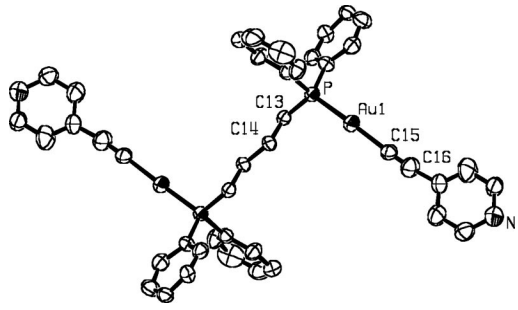

Figure 6. Molecular structure of $[Au_2(C{\equiv}CC_5H_4N)_2(\mu_2\text{-dppb})]$(**7**).

Table 5. Selected bond lengths [Å] and angles [°] of **7**.

Au1–P	2.2761(16)	P–Au1–C15	177.63(15)
Au1–C15	2.122(6)	Au1–C15–C16	169.5(6)
C15–C16	1.110(10)	Au1–P–C13	113.17(17)
		P–C13–C14	111.0(4)

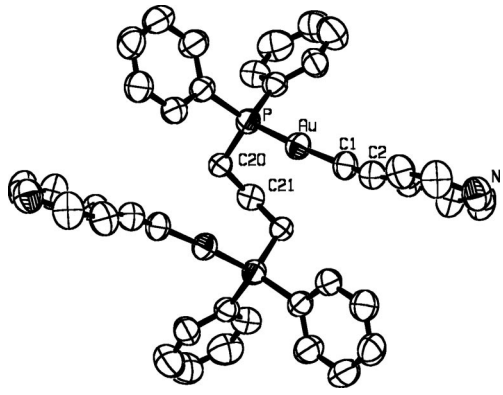

Figure 7. Molecular structure of $[Au_2(C{\equiv}CC_5H_4N)_2(\mu_2\text{-dppp})]$(**6**).

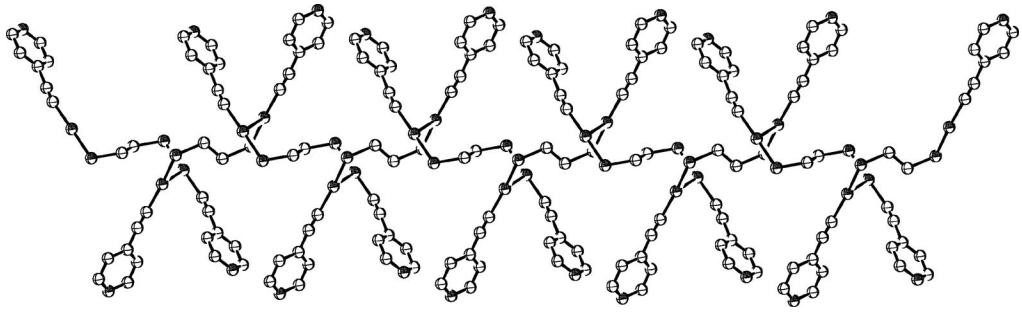

Figure 5. Supramolecular association in **5** through intermolecular aurophilic contacts to form an infinite chain.

Table 6. Selected bond lengths [Å] and angles [°] of **9**.

Au1···Au2	3.3772(13)	P1–Au1–C11	177.1(3)
Au1–P1	2.284(2)	Au1–C11–C12	167.9(12)
Au1–C11	2.021(11)	P2–Au2–C21	177.0(3)
Au2–P2	2.299(3)	Au2–C21–C22	179.5(13)
Au2–C21	2.055(15)	C2–P1–Au1	112.9(3)
Au3–P3	2.287(3)	C3–P2–Au2	116.8(3)
Au3–C31	2.011(11)	C11–Au1···Au2	98.3(3)
C11–C12	1.181(16)	P1–Au1···Au2	80.12(6)
C21–C22	1.139(18)	C21–Au2···Au1	103.9(3)
C31–C32	1.204(16)	P2–Au2···Au1	78.33(6)
		P3–Au3–C31	173.2(3)
		Au3–C31–C32	166.0(11)
		C4–P3–Au3	114.6(3)
		C2–C1–C3	113.2(8)

The molecular structure of triphos compound **9** (Figure 8) shows aurophilic contacts [*d*(Au···Au) = 3.3772(13) Å] between the gold atoms corresponding to two of the arms of the triphosphane, whereas the third one lies apart. This asymmetric disposition is similar to that found for the closely related compounds [Au_3X_3(μ_3-triphos)] (X = Cl)[52] (X = Br, I).[53] The crystal packing is determined by the existence of weak N···Au interactions [3.114(11) Å] between the nitrogen atom of the pyridine ring that belongs to one of the arms involved in the intramolecular interaction and the gold atom of a neighbouring molecule not involved in the named interaction. The chains are parallel to the *c* axis and are shown in Figure 9. Some reports can be found where N···Au contacts have a decisive influence on the lattice organisation; for example, the compound [AuCl(2-diphenylphosphanylpicolinamide)],[54] where *d*(N···Au) = 3.129 Å, adopts a lattice distribution analogous to that of compound **9** and the complex [Au(tht)$_2$][$C_6H_4NO_4S_2$][55] displays a *d*(N···Au) = 3.009 Å.

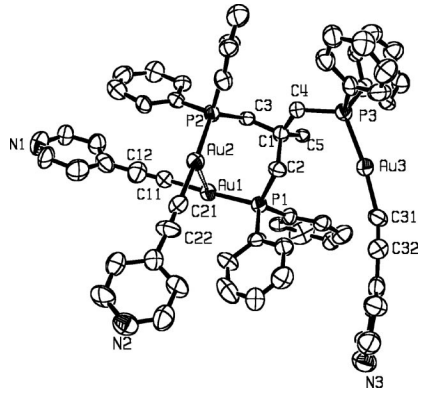

Figure 8. Molecular structure of [Au_3(C≡CC_5H_4N)$_3$(μ_3-triphos)](**9**).

The use of phosphanes with different backbones has allowed us to obtain a wide range of structures (molecules with no interactions, molecules with intramolecular interactions, molecules that form discrete dimers and molecules that assemble into polymeric chains by intermolecular interactions), depending on the nature of the phosphane bridging chain. Although complexes with phosphane ligands that have restricted rotation due to the small bite angle between phosphorus atoms (dppip **3**, triphos **9**) displayed intramolecular Au···Au contacts, diphosphanes with conformationally flexible backbones (dppe **5**, dppp **6**, dppb **7**) crystallise with the alkane chain fully extended and, in some cases, intermolecular Au···Au interactions link up the gold complexes to form extended chains (dppe **5**). A particular case is the formation of a dimer through intermolecular interactions for the conformationally inflexible dppa derivative **4**, a fact that could be attributable to packing forces.

Fortunately, the diversity of the obtained structures offered us a good opportunity to study in detail the photophysical properties of the compounds in order to find correlations between the observed absorption and emission trends and the presence and nature of aurophilic contacts.

Photophysical Studies

The electronic absorption spectra of compounds **1**–**9** were recorded in dichloromethane solution at room temperature. The results are summarised in Table 7.

All the complexes exhibit intense high-energy absorptions in the range 250–300 nm, which in some cases present a tail extending to ca. 370 nm. The band at ca. 250 nm, which is also present in the free diphosphane ligands, has been assigned as a phosphane-centred intraligand transition. The intense and vibronically structured electronic absorption in the range 267–286 nm, with progressional spacings of ca. 1860 cm^{-1}, typical of ν(C≡C) stretching frequencies in the excited state, is assigned to intraligand (IL) π→π* (C≡Cpy), as seen in other published works on alkynyl gold(I) phosphane complexes.[25,26,56–58] This attribution is also confirmed by the observation of conformation-dependent excitonic perturbations (see below).

In order to minimise the possibility of the establishment of aurophilic intermolecular interactions in solution, absorption spectra of these complexes (Figure 10a) were carried out at diluted concentrations (10^{-6} M). Compounds **1**–**3**, **5**–**7** and **9**, which contain the same chromophoric units but different numbers of carbon atoms at the alkyl bridging chain, are expected to present identical absorption spectra, unless different interactions occur at the molecular level.

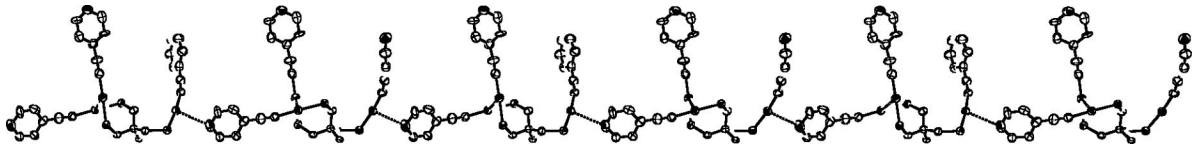

Figure 9. Supramolecular association in **9** through intermolecular N···Au interactions to form an infinite chain.

Table 7. Electronic absorption (10^{-6} M freshly prepared dichloromethane solution, room temp.) and emission data in the solid state (room temp.) for compounds **1**–**9**.

Compound	Absorption data λ_{abs} [nm] ($10^{-3}\varepsilon$, $M^{-1}cm^{-1}$)	Emission data (λ_{ex} = 360 nm) λ_{em} [nm] (τ, μs)
1	252 (24.9), 268 (32.6), 282 (35.4)	405, 428, 444, 462 (36)
2	271 (40.5), 286 sh. (36.0)	458 (1.1)
3	272 (43.6), 284 sh. (39.3)	420, 440, 458, 516 (1.5)
4	252 sh. (48.7), 268 (56.9), 284 (61.0)	530 (0.7)
5	253 (30.8), 267 (49.1), 282 (56.3)	505 (1.2)
6	254 (30.5), 267 (54.6), 282 (59.7)	407, 427, 442, 547[a] (3.5)
7	252 (29.8), 268 (56.9), 281 (65.4)	410, 441, 456, 503 (3.5)
8	252 (46.1), 268 (57.9), 282 (62.3)	nonemissive
9	251 (55.4), 268 (77.7), 282 (86.3)	508, 570 sh. (1.7)

[a] From gated emission spectra with 50 μs delay after excitation with a pulsed Xenon lamp (ca. 40 μs pulse width).

Although compounds **4** and **8** have additional chromophores, they do not modify the position of the observed bands. Although compounds **1** and **4**–**8** exhibit identical features (two well-resolved peaks with maxima at ca. 268 and 282 nm), the corresponding spectra of **2** (dppm) and **3** (dppip) display different characteristics: a broad band with a maximum at ca. 272 and shoulder at ca. 285 nm with a tail at longer wavelengths. A special case is the spectrum of compound **9** (triphos), which seems to present a mixture of both features (representative examples are shown in Figure 10b).

It is interesting to notice that compounds **2** and **3** are also different from the other compounds in the homochromophoric series, as their ^{13}C NMR spectra seem to indicate the presence of intramolecular aurophilic interactions in solution (see above). Moreover, the X-ray crystal structure of compound **3** shows the presence of a rather short intramolecular gold–gold contact [3.235(2) Å].

It is well known, for dimers in solution, that interaction between the transition dipoles leads to the appearance of new excitonic transitions and a consequent broadening of the absorption spectra when compared to monomer absorption.[59] The observed broadening in the absorption bands of compounds **2** and **3** strongly suggests the existence of intramolecular aurophilic interactions that could be responsible for a molecular conformation where the two ethynylpyridine ligands are close enough to strongly interact and undergo exciton splitting. A similar effect was pointed out for other alkynyl gold(I) compounds bearing Au–Au interactions.[31]

In the case of compound **9**, despite the fact that the UV/Vis spectrum clearly shows an excitonic perturbation, its interpretation is not straightforward, as its corresponding NMR spectra (^{31}P, ^{1}H and ^{13}C), even at low temperature, show the equivalence of the three arms of the triphosphane. The X-ray crystal structure, however, displays an intramolecular aurophilic interaction between a pair of gold(I) atoms.

Analysis of the dependence of the extinction coefficients on the nuclearity of the complexes shows that for diphosphane compounds **4**–**8**, the molar absorptivities are roughly twice those of triphenylphosphane compound **1**, whereas for **2** and **3** the values are slightly lower, as expected for the observed excitonic broadening. The latter effect is also observed for triphos compound **9**, whose extinction coefficients are a bit lower than the expected triple.

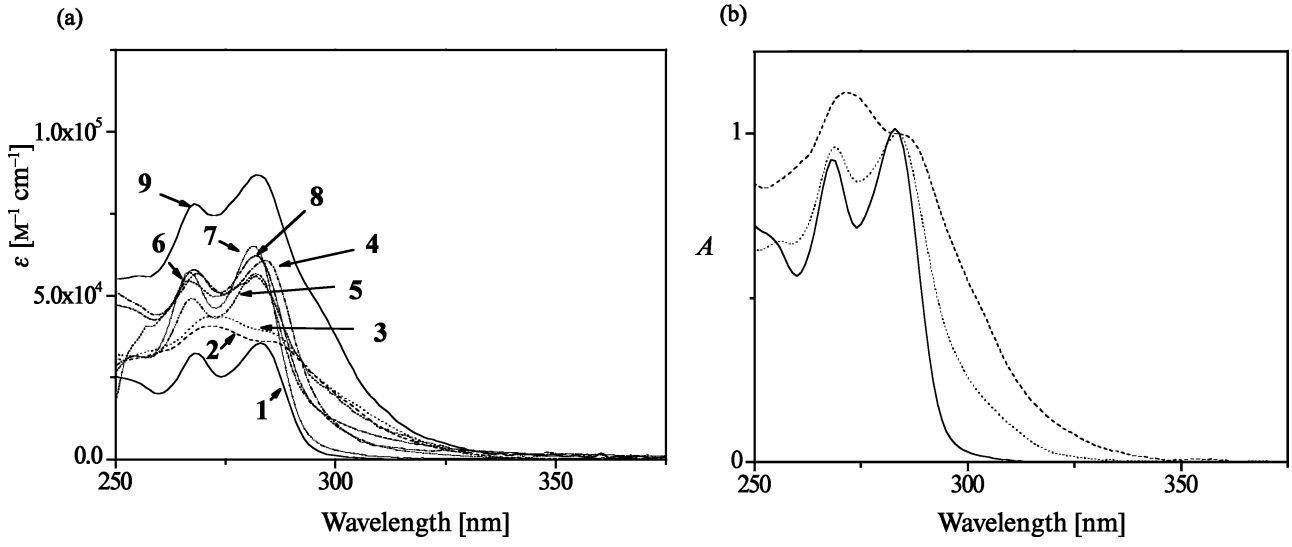

Figure 10. (a) Electronic absorption spectra of compounds **1**–**9** in dichloromethane (10^{-6} M), (b) normalised electronic absorption spectra of compounds **1** (solid line), **2** (dashed line) and **9** (dotted line) in dichloromethane.

The emission of the complexes in dichloromethane solution is very weak and the compounds undergo rapid photodecomposition during the tracing of the emission spectrum. This behaviour was also reported for other alkynyl gold(I) complexes.[9]

The excitation of the solids with λ = 360 nm at room temperature produces intense emission bands between 425 and 570 nm (Table 7) for compounds **1**–**7** and **9**, whereas the luminescence of compound **8** is strongly quenched by the presence of the ferrocenyl group.[50,57,60] The observed large Stokes shifts suggest a triplet parentage for the excited state and, therefore, phosphorescence emissions. The band at higher energies (in the range 425–458 nm) displays a well-defined vibrational structure, whereas the band at lower energies (in the range 500–570 nm) presents a broad structureless shape (Figure 11). This fact together with the difference in the excitation spectra monitored at the high- and low-energy emission bands are indicative of different origins for the corresponding emissions.

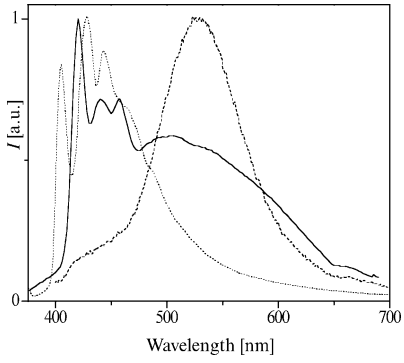

Figure 11. Solid-state emission spectra of compounds **1** (dotted line), **3** (solid line) and **4** (dashed line) upon excitation at λ = 360 nm at room temperature.

The excitation spectra monitored at the high-energy emission bands reproduces absorption spectra bands in the range 250–300 nm, which is consistent with an emission of ligand-centred origin. Moreover, the vibronic structure of these bands is also indicative of the involvement of the ligands in the transition. Thus, by comparison with the literature,[26,57] we assign the high-energy emission band displayed by our complexes to an intraligand ^{3}[π-π*(alkynyl)] emission.

In contrast, excitation spectra collected for all the compounds at 500–600 nm display a band at ca. 360 nm (Stokes shift ca. 8000 cm^{-1}), which is not clearly visible in the absorption spectra of diluted solutions collected in 1-cm path cells. However, absorption spectra of the same solutions obtained in 10 cm path cells clearly display the 360 nm absorption band. These broad emissions are usually assigned as derived from the ^{3}[σ(Au–P)→π*(C≡Cpy)] excited state,[6,25,57] although a contribution of Au-centred states to their origin should not be ruled out.[11,56,58,61]

The two emission bands present different proportions depending on the complex. Although for compounds **1** and **6** the structured band is predominant, the broad band at lower energy dominates the emission of compounds **2**, **4** and **5**. Compounds **3** and **7** present similar contributions of these two bands (see Supporting Information). Figure 11 shows illustrative examples of the different emission patterns. In fact, the phosphorescence spectrum of compound **6**, collected with a delay between excitation and emission of 50 μs, is completely different from the one obtained without delay showing a broad emission band centred at 547 nm instead of the high-energy structured band (Figure 12).

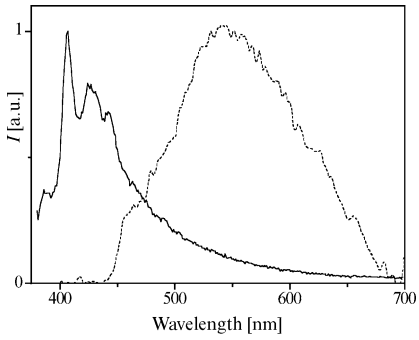

Figure 12. Time-gated emission spectra (normalised) of compound **6** (solid) recorded at room temperature: without delay time (solid line) and with 50 μs delay after excitation (dashed line).

Compound **9** is a particular case because the low-energy transition is split into two broad emission bands at 508 and 570 nm that we suspect to correlate with two different environments of gold atoms. This is in agreement with the X-ray data, which show intramolecular aurophilic interaction between two of the three arms; a fact that could have an influence on the emission.

Our results seems to indicate that aurophilic interactions are not a prerequisite for the observation of a broad emission band at lower energies, as the spectra of dppip derivative **3** and dppb derivative **7**, whose X-ray structures show intramolecular and no gold–gold contacts, respectively, show similar profiles. At the same time, careful analysis of the emission spectra does not show any correlation between the existence of gold–gold contacts and the position and/or the intensity of the emission bands.[50,62]

Conclusions

We report here the synthesis and characterisation of new alkynyl gold(I) phosphane compounds derived from the ethynylpyridine. The use of phosphanes with different carbon-chain features allowed us to structurally characterise a series of compounds that adopt a wide variety of structural motifs, which, in some cases, are the result of the establishment of intra- or intermolecular aurophilic interactions.

From the photophysical measurements, it was found that absorption band broadening could be indicative of the existence of intramolecular aurophilic interactions in solution. In contrast, the emission and excitation spectra of the complexes in the solid state did not display significant differences, independently of the presence or absence of either intra- or intermolecular gold–gold interactions. As a consequence, we can conclude that there is not a straightforward

relation between the existence of Au···Au interactions and the occurrence and/or characteristics of the broad low-energy emission band displayed by alkynyl gold(I) phosphane complexes.

Experimental Section

General Procedures: All manipulations were performed under prepurified N_2 by using standard Schlenk techniques. All solvents were distilled from appropriate drying agents. Commercial reagents PPh_3, dppa, dppbz, dppf, dppp and 4-bromopyridine hydrochloride were used as received. Literature methods were used to prepare [AuCl(tht)],[63] $[Au(C{\equiv}CC_5H_4N)]_n$,[4] $NC_5H_4C{\equiv}CH$,[64] dppm,[65] dppip,[32] dppe[65] and dppb.[65]

Physical Measurements: Infrared spectra were recorded with a FTIR 520 Nicolet spectrophotometer. ^1H NMR [δ(TMS) = 0.0 ppm], $^{31}P\{^1H\}$ NMR [δ(85% H_3PO_4) = 0.0 ppm] and $^{13}C\{^1H\}$ NMR [δ(TMS) = 0.0 ppm] spectra were obtained with a Varian Unity 400 and Bruker DXR 250 spectrometers at 25 °C unless otherwise stated. The g-NMR software package was used to simulate NMR spectroscopic data. Elemental analyses of C, H and N were carried out at the Serveis Científico-Tècnics in Barcelona. MS (ESI) spectra were recorded with a Fisons VG Quatro spectrometer. Absorption spectra were recorded with a Shimadzu UV-2501PC spectrophotometer and emission spectra with a Horiba-Jobin–Yvon SPEX Fluorolog 3.22 spectrofluorimeter. The decay times of the powders were measured with a laser flash photolysis LK60 Applied Photophysics system in emission mode, collecting the decay at 550 nm after laser pulse excitation at 355 nm.

$[Au(C{\equiv}CC_5H_4N)(PPh_3)]$ (1): To a suspension of $[Au(C{\equiv}CC_5H_4N)]_n$ (50 mg, 0.17 mmol) in CH_2Cl_2 (15 mL) was added solid PPh_3 (44 mg, 0.17 mmol), and the mixture was stirred for 1 h and then filtered through Celite. The resulting solution was concentrated (5 mL) and diethyl ether (10 mL) was added to precipitate a white solid. Yield: 80 mg, 85%. ^1H NMR (400.1 MHz, $CDCl_3$): δ = 8.47 (d, J = 5.6 Hz, 2 H, $H_{\alpha\text{-pyr}}$), 7.57–7.45 (m, 15 H, PPh_3), 7.32 (d, J = 6.0 Hz, 2 H, $H_{\beta\text{-pyr}}$) ppm. $^{13}C\{^1H\}$ NMR (100.0 MHz, $CDCl_3$): δ = 149.5 (s, $C_{\alpha\text{-pyr}}$), 134.4 (d, J = 14 Hz, C_{ortho} Ph), 133.2 (s, $C_{\gamma\text{-pyr}}$), 131.8 (s, J = 2 Hz, C_{para} Ph), 129.5 (d, J = 56 Hz, C_{ipso} Ph), 129.3 (d, J = 11 Hz, C_{meta} Ph), 126.6 (s, $C_{\beta\text{-pyr}}$), 101.5 (s, P-Au-C≡*C*) ppm. $^{31}P\{^1H\}$ NMR (101.2 MHz, $CDCl_3$): δ = 42.5 (s, PPh_3) ppm. $C_{25}H_{19}AuNP$ (561.37): calcd. C 53.49, H 3.41, N 2.50; found C 53.57, H 3.31, N 2.55. IR (KBr): $\tilde{\nu}$ = 2120 (C≡C) cm^{-1}. MS (ESI): m/z = 562.1 $[M + H]^+$.

$[Au_2(C{\equiv}CC_5H_4N)_2(\mu_2\text{-dppm})]$ (2): To a suspension of $[Au(C{\equiv}CC_5H_4N)]_n$ (50 mg, 0.17 mmol) in CH_2Cl_2 (15 mL) was added solid dppm (32 mg, 0.08 mmol), and the mixture was stirred for 1 h and then filtered through Celite. The resulting solution was concentrated (5 mL) and *n*-hexane (20 mL) was added to precipitate a white solid. The compound was recrystallised from CH_2Cl_2/*n*-hexane. Yield: 60 mg, 73%. ^1H NMR (400.1 MHz, $CDCl_3$): δ = 8.35 (d, J = 5.2 Hz, 4 H, $H_{\alpha\text{-pyr}}$), 7.65–7.33 (m, 20 H, PPh_2), 7.25 (d, J = 5.2 Hz, 4 H, $H_{\beta\text{-pyr}}$), 3.60 (t, J = 10.9 Hz, 2 H, P-CH_2-P) ppm. $^{13}C\{^1H\}$ NMR (100.0 MHz, $CDCl_3$): δ = 149.4 (s, $C_{\alpha\text{-pyr}}$), 140.5 (AXX′ m, $^2J_{calcd.} \approx 140$ Hz, $^{3+4}J_{calcd.} \approx 4$ Hz, P-Au-*C*≡C), 133.6 (t, C_{ortho} Ph), 132.6 (s, $C_{\gamma\text{-pyr}}$), 132.4 (s, C_{para} Ph), 129.6 (s, C_{meta} Ph), 129.2 (t, C_{ipso} Ph), 126.7 (s, $C_{\beta\text{-pyr}}$), 102.5 (AXX′ t, $^3J_{calcd.} \approx 20$ Hz, $^{4+5}J_{calcd.} \approx 3$ Hz, P-Au-C≡*C*), 29.7 (t, J = 26 Hz, P-*C*H_2-P) ppm. $^{31}P\{^1H\}$ NMR (101.2 MHz, $CDCl_3$): δ = 30.8 (s, d) ppm. IR (KBr): $\tilde{\nu}$ = 2107 (C≡C) cm^{-1}. MS (ESI): m/z = 983.1 $[M + H]^+$, 492.3 $[M + 2H]^{2+}$. $C_{39}H_{30}Au_2N_2P_2$ (982.56): calcd. C 47.67, H 3.08, N 2.85; found C 47.71, H 3.11, N 2.90.

$[Au_2(C{\equiv}CC_5H_4N)_2(\mu_2\text{-dppip})]$ (3): Derivative **3** was prepared according to the procedure outlined for **2**. Yield: 65 mg, 80%. ^1H NMR (400.1 MHz, $CDCl_3$): δ = 8.35 (d, J = 6.0 Hz, 4 H, $H_{\alpha\text{-pyr}}$), 7.92–7.39 (m, 24 H, PPh_2, $H_{\beta\text{-pyr}}$), 1.70 [t, J = 14.8 Hz, 6 H, P-$C(CH_3)_2$-P] ppm. $^{13}C\{^1H\}$ NMR (100.0 MHz, $CDCl_3$): δ = 149.3 (s, $C_{\alpha\text{-pyr}}$), 140.8 (AXX′ m, $^2J_{calcd.} \approx 150$ Hz, $^{3+4}J_{calcd.} \approx -15$ Hz, P-Au-*C*≡C), 136.4 (t, C_{ortho} Ph), 134.0 (s, $C_{\gamma\text{-pyr}}$), 132.4 (s, C_{para} Ph), 129.2 (t, C_{meta} Ph), 127.0 (t, C_{ipso} Ph), 126.8 (s, $C_{\beta\text{-pyr}}$), 102.4 (AXX′ t, $^2J_{calcd.} \approx 20$ Hz, $^{3+4}J_{calcd.} \approx 2$ Hz, P-Au-C≡*C*), 40.3 [t, J = 22 Hz, P-*C*$(CH_3)_2$-P], 25.1 [s, P-C(*C*$H_3)_2$-P] ppm. $^{31}P\{^1H\}$ NMR (101.2 MHz, $CDCl_3$): δ = 56.7 (s, dppip) ppm. IR (KBr): $\tilde{\nu}$ = 2120 (C≡C) cm^{-1}. MS (ESI): m/z = 1011.4 $[M + H]^+$, 506.2 $[M + 2H]^{2+}$. $C_{41}H_{34}Au_2N_2P_2$ (1010.61): calcd. C 48.73, H 3.39, N 2.77; found C 48.77, H 3.45, N 2.83.

$[Au_2(C{\equiv}CC_5H_4N)_2(\mu_2\text{-dppa})]$ (4): Derivative **4** was prepared according to the procedure outlined for **2**. Yield: 50 mg, 63%. ^1H NMR (400.1 MHz, $CDCl_3$): δ = 8.49 (d, J = 6.0 Hz, 4 H, $H_{\alpha\text{-pyr}}$), 7.76–7.46 (m, 20 H, PPh_2), 7.30 (d, J = 6.0 Hz, 4 H, $H_{\beta\text{-pyr}}$) ppm. $^{13}C\{^1H\}$ NMR (100.0 MHz, $CDCl_3$): δ = 149.6 (s, $C_{\alpha\text{-pyr}}$), 136.5 (s, P-Au-*C*≡C), 133.4 (d, J = 16 Hz, C_{ortho} Ph), 132.9 (s, $C_{\gamma\text{-pyr}}$), 132.4 (d, J = 2 Hz, C_{para} Ph), 129.8 (d, J = 12 Hz, C_{meta} Ph), 128.6 (d, J = 53 Hz, C_{ipso} Ph), 126.6 (s, $C_{\beta\text{-pyr}}$), 102.5 (br. d, J = 16 Hz P-C≡C-P), 101.6 (s, P-Au-C≡*C*) ppm. $^{31}P\{^1H\}$ NMR (101.2 MHz, $CDCl_3$): δ = 16.6 (s, dppa) ppm. $C_{40}H_{28}Au_2N_2P_2$ (992.56): calcd. C 48.40, H 2.84, N 2.82; found C 48.41, H 2.91, N 2.87. IR (KBr): $\tilde{\nu}$ = 2120 (C≡C) cm^{-1}. MS (ESI): m/z = 993.1 $[M + H]^+$, 497.2 $[M + 2H]^{2+}$.

$[Au_2(C{\equiv}CC_5H_4N)_2(\mu_2\text{-dppe})]$ (5): Derivative **5** was prepared according to the procedure outlined for **2**. Yield: 60 mg, 75%. ^1H NMR (400.1 MHz, $CDCl_3$): δ = 8.47 (d, J = 5.6 Hz, 4 H, $H_{\alpha\text{-pyr}}$), 7.65–7.44 (m, 20 H, PPh_2), 7.30 (d, J = 6.0 Hz, 4 H, $H_{\beta\text{-pyr}}$), 2.65 (s, 4 H, P-CH_2CH_2-P) ppm. $^{13}C\{^1H\}$ NMR (100.0 MHz, $CDCl_3$): δ = 149.7 (s, $C_{\alpha\text{-pyr}}$), 140.3 (br. d, J = 142 Hz, P-Au-*C*≡C), 133.6 (t, C_{ortho} Ph), 133.1 (s, $C_{\gamma\text{-pyr}}$), 132.6 (s, C_{para} Ph), 129.8 (t, C_{meta} Ph), 128.7 (t, C_{ipso} Ph), 126.7 ($C_{\beta\text{-pyr}}$), 101.8 (br. s, P-Au-C≡*C*), 24.2 (t, P-*C*H_2*C*H_2-P) ppm. $^{31}P\{^1H\}$ NMR (101.2 MHz, $CDCl_3$): δ = 40.1 (s, dppe) ppm. $C_{40}H_{32}Au_2N_2P_2$ (996.59): calcd. C 48.21, H 3.24, N 2.81; found C 48.28, H 3.29, N 2.86. IR (KBr): $\tilde{\nu}$ = 2117 (C≡C) cm^{-1}. MS (ESI): m/z = 997.1 $[M + H]^+$, 499.1 $[M + 2H]^{2+}$.

$[Au_2(C{\equiv}CC_5H_4N)_2(\mu_2\text{-dppp})]$ (6): Derivative **6** was prepared according to the procedure outlined for **2**. Yield: 65 mg, 80%. ^1H NMR (400.1 MHz, $CDCl_3$): δ = 8.49 (d, J = 6.0 Hz, 4 H, $H_{\alpha\text{-pyr}}$), 7.72–7.42 (m, 20 H, PPh_2), 7.30 (d, J = 6.0 Hz, 4 H, $H_{\beta\text{-pyr}}$), 2.84 (m, 4 H, P-CH_2-CH_2-CH_2-P), 1.95 (m, 2 H, P-CH_2-CH_2-CH_2-P) ppm. $^{13}C\{^1H\}$ NMR (100.0 MHz, $CDCl_3$): δ = 149.7 (s, $C_{\alpha\text{-pyr}}$), 140.1 (d, J = 140 Hz, P-Au-*C*≡C), 133.7 (d, J = 13 Hz, C_{ortho} Ph), 133.4 (s, $C_{\gamma\text{-pyr}}$), 132.1 (d, J = 2 Hz C_{para} Ph), 129.6 (d, J = 11 Hz, C_{meta} Ph), 129.5 (d, J = 54 Hz, C_{ipso} Ph), 126.6 (s, $C_{\beta\text{-pyr}}$), 101.9 (d, J = 26 Hz, P-Au-C≡*C*), 28.9 (dd, ^1J = 34 Hz, ^3J = 11 Hz, P-*C*H_2-CH_2-*C*H_2-P), 20.3 (t, J = 4 Hz, P-CH_2-*C*H_2-CH_2-P) ppm. $^{31}P\{^1H\}$ NMR (101.2 MHz, $CDCl_3$): δ = 32.4 (s, dppp) ppm. $C_{41}H_{34}Au_2N_2P_2$ (1010.61): calcd. C 48.73, H 3.39, N 2.77; found C 48.61, H 3.41, N 2.81. IR (KBr): $\tilde{\nu}$ = 2120 (C≡C) cm^{-1}. MS (ESI): m/z = 1011.2 $[M + H]^+$, 506.1 $[M + 2H]^{2+}$.

$[Au_2(C{\equiv}CC_5H_4N)_2(\mu_2\text{-dppb})]$ (7): Derivative **7** was prepared according to the procedure outlined for **2**. Yield: 70 mg, 85%. ^1H NMR (400.1 MHz, $CDCl_3$): δ = 8.49 (d, J = 6.0 Hz, 4 H, $H_{\alpha\text{-pyr}}$), 7.67–7.44 (m, 20 H, PPh_2), 7.32 (d, J = 6.0 Hz, 4 H, $H_{\beta\text{-pyr}}$), 2.41 [m, 4 H, P-CH_2-$(CH_2)_2$-CH_2-P], 1.79 [m, 4 H, P-CH_2-(C$H_2)_2$-CH_2-P] ppm. $^{13}C\{^1H\}$ NMR (100.0 MHz, $CDCl_3$): δ = 149.7 (s, $C_{\alpha\text{-pyr}}$), 140.4 (d, J = 141 Hz, P-Au-*C*≡C), 133.5 (d, J = 13 Hz, C_{ortho} Ph), 133.3 (s, $C_{\gamma\text{-pyr}}$), 132.1 (s, C_{para} Ph), 129.9 (d, J = 60 Hz, C_{ipso} Ph),

129.6 (d, J = 11 Hz, C_{meta} Ph), 126.7 (s, $C_{\beta\text{-pyr}}$), 101.6 (d, J = 26 Hz, P-Au-C≡*C*), 28.0 [d, J = 34 Hz, P-*C*H$_2$-(CH$_2$)$_2$-*C*H$_2$-P], 27.3 [d, J = 17 Hz, P-CH$_2$-(*C*H$_2$)$_2$-CH$_2$-P] ppm. ^{31}P{^{1}H} NMR (101.2 MHz, $CDCl_3$): δ = 37.4 (s, dppb) ppm. $C_{42}H_{36}Au_2N_2P_2$ (1024.64): calcd. C 49.23, H 3.54, N 2.73; found C 49.31, H 3.51, N 2.79. IR (KBr): $\tilde{\nu}$ = 2120 (C≡C) cm^{-1}. MS (ESI): m/z = 1025.1 [M + H]$^+$, 513.2 [M + 2H]$^{2+}$.

[Au$_2$(C≡CC$_5$H$_4$N)$_2$(μ$_2$-dppf)] (8): Derivative **8** was prepared according to the procedure outlined for **2**. Yield: 65 mg, 70%. ^{1}H NMR (400.1 MHz, $CDCl_3$): δ = 8.48 (d, J = 6.4 Hz, 4 H, $H_{\alpha\text{-pyr}}$), 7.56–7.40 (m, 20 H, P*Ph*$_2$), 7.32 (d, J = 6.4 Hz, 4 H, $H_{\beta\text{-pyr}}$), 4.72 (br. s, 4 H, 2,5-H C$_5$H$_4$), 4.33 (br. s, 4 H, 3,4-H C$_5$H$_4$) ppm. ^{13}C{^{1}H} NMR (100.0 MHz, $CDCl_3$): δ = 149.7 (s, $C_{\alpha\text{-pyr}}$), 139.5 (d, J = 144 Hz, P-Au-*C*≡C), 133.8 (d, J = 14 Hz, C_{ortho} Ph), 133.4 (s, $C_{\gamma\text{-pyr}}$), 131.8 (s, J = 2 Hz, C_{para} Ph), 131.2 (d, J = 58 Hz, C_{ipso} Ph), 129.3 (d, J = 11 Hz, C_{meta} Ph), 126.7 (s, $C_{\beta\text{-pyr}}$), 101.8 (d, J = 27 Hz, P-Au-C≡*C*), 75.2 (s, C-3,4 C$_5$H$_4$), 75.1 (d, J = 5 Hz, C-2,4 C$_5$H$_4$), 72.1 (d, J = 64 Hz, C-1 C$_5$H$_4$) ppm. ^{31}P{^{1}H} NMR (101.2 MHz, $CDCl_3$): δ = 36.9 (s, dppf) ppm. IR (KBr): $\tilde{\nu}$ = 2120 (C≡C) cm^{-1}. MS (ESI): m/z = 1153.0 [M + H]$^+$, 577.2 [M + 2H]$^{2+}$. $C_{48}H_{36}Au_2FeN_2P_2$ (1152.55): calcd. C 50.02, H 3.15, N 2.43; found C 50.11, H 3.19, N 2.53.

[Au$_3$(C≡CC$_5$H$_4$N)$_3$(μ$_3$-triphos)] (9): To a suspension of [Au(C≡CC$_5$H$_4$N)]$_n$ (50 mg, 0.17 mmol) in CH_2Cl_2 (15 mL) was added solid triphos (31 mg, 0.05 mmol), and the mixture was stirred for 1 h and then filtered through Celite. The resulting solution was concentrated (5 mL) and *n*-hexane (20 mL) was added to precipitate a white solid. The compound was recrystallised from CH_2Cl_2/*n*-hexane. Yield: 60 mg, 79%. ^{1}H NMR (400.1 MHz, $CDCl_3$): δ = 8.48 (d, J = 5.6 Hz, 6 H, $H_{\alpha\text{-pyr}}$), 7.89–7.41 (m, 30 H, P*Ph*$_2$), 7.22 (d, J = 6.0 Hz, 6 H, $H_{\beta\text{-pyr}}$), 3.40 (d, J = 10.8 Hz, 6 H, CH_2), 0.85 (s, 3 H, CH_3) ppm. ^{13}C{^{1}H} NMR (100.0 MHz, $CDCl_3$): δ = 149.7 (s, $C_{\alpha\text{-pyr}}$), 139.5 (d, J = 139 Hz, P-Au-*C*≡C), 134.1 (d, J = 14 Hz, C_{ortho} Ph), 133.3 (s, $C_{\gamma\text{-pyr}}$), 132.2 (s, C_{para} Ph), 130.9 (d, J = 55 Hz, C_{ipso} Ph), 129.7 (d, J = 11 Hz, C_{meta} Ph), 126.6 (s, $C_{\beta\text{-pyr}}$), 101.9 (d, J = 26 Hz, P-Au-C≡*C*), 42.9 (dt, ^1J = 30 Hz, ^3J = 7 Hz, CH_2), 39.0 (s, CH_3), 30.9 (q, ^2J = 6 Hz, *C*-CH$_3$) ppm. ^{31}P{^{1}H} NMR (101.2 MHz, $CDCl_3$): δ = 25.5 (s, triphos) ppm. IR (KBr): $\tilde{\nu}$ = 2120 (C≡C) cm^{-1}. MS (ESI): m/z = 1523.1 [M + H]$^+$, 761.9 [M + 2H]$^{2+}$, 508.3 [M + 3H]$^{3+}$. $C_{62}H_{51}Au_3N_3P_3$ (1521.23): calcd. C 48.93, H 3.38, N 2.76; found C 48.96, H 3.41, N 2.80.

[Au(dppbz)$_2$] [Au(C≡CC$_5$H$_4$N)$_2$] (10): To a suspension of [Au(C≡CC$_5$H$_4$N)]$_n$ (50 mg, 0.17 mmol) in CH_2Cl_2 (15 mL) was added solid dppbz (75 mg, 0.17 mmol), and the mixture was stirred for 1 h and then filtered through Celite. The resulting solution was concentrated (5 mL) and diethyl ether (20 mL) was added to precipitate a yellow solid. Yield: 80 mg, 63%. ^{1}H NMR (400.1 MHz, $CDCl_3$): δ = 8.29 (d, J = 5.2 Hz, 4 H, $H_{\alpha\text{-pyr}}$), 7.54–7.43 (m, 8 H, P-C$_6$H$_4$-P), 7.32 (m, 8 H, H_{para} P*Ph*$_2$), 7.23 (d, J = 5.6 Hz, 4 H, $H_{\beta\text{-pyr}}$), 7.10–7.00 (m, 32 H, $H_{meta+ortho}$ P*Ph*$_2$) ppm. ^{13}C{^{1}H} NMR (100.0 MHz, $CDCl_3$): δ = 149.1 (s, $C_{\alpha\text{-pyr}}$), 142.2 (AXX′X′′$_2$ m, $^1J_{calcd.}$ ≈ 35 Hz, $^2J_{calcd.}$ ≈ 4 Hz, C_{ipso} P-C$_6$H$_4$-P), 135.9 (s, $C_{\gamma\text{-pyr}}$), 134.4 (m, C-3,4 P-C$_6$H$_4$-P), 132.6 (AXX′X′′$_2$ m, C_{ipso} P*Ph*$_2$), 132.4 (m, C_{ortho} P*Ph*$_2$), 131.8 (s, C-5,6 P-C$_6$H$_4$-P), 130.5 (s, C_{para} P*Ph*$_2$), 129.2 (m, C_{meta} P*Ph*$_2$), 127.0 (s, $C_{\beta\text{-pyr}}$), 100.9 (s, P-Au-C≡*C*) ppm. ^{31}P{^{1}H} NMR (101.2 MHz, $CDCl_3$): δ = 21.7 (s, dppbz) ppm. IR (KBr): $\tilde{\nu}$ = 2103 (C≡C) cm^{-1}. MS (ESI+): m/z (%) = 1089.2 [Au(dppbz)$_2$]$^+$. MS (ESI–): m/z (%) = 401.3 [Au(C≡CC$_5$H$_4$N)$_2$]$^-$. $C_{74}H_{58}Au_2N_2P_4$ (1493.12): calcd. C 59.53, H 3.91, N 1.88; found C 59.59, H 3.94, N 1.91.

Table 8. Crystal and structure determination data.

Compound	**3**	**4**	**5**·0.5CHCl$_3$
Empirical formula	$C_{41}H_{34}Au_2N_2P_2$	$C_{80}H_{56}Au_4N_4P_4$	$C_{40}H_{32}Au_2N_2P_2$
Formula weight	1010.58	1985.03	1056.23
Temperature [K]	293(2)	293(2)	293(2)
Wavelength [Å]	0.71073	0.71073	0.71073
Crystal system	triclinic	triclinic	triclinic
Space group	$P\bar{1}$	$P\bar{1}$	$P\bar{1}$
a [Å]	11.315(5)	12.546(7)	12.622(9)
b [Å]	14.579(16)	12.882(5)	13.086(13)
c [Å]	22.790(5)	12.987(7)	14.774(4)
α [°]	81.34(4)	87.34(3)	112.61(4)
β [°]	82.50(3)	70.99(3)	93.52(4)
γ [°]	71.70(6)	61.330(2)	114.42(6)
V [Å^3]	3515(4)	1725.8(15)	1979(2)
Z	4	1	2
$D_{calcd.}$ [Mg m^{-3}]	1.910	1.910	1.772
Absorption coefficient [mm^1]	8.462	8.615	7.615
F(000)	1928	940	1006
Crystal size [mm]	0.09 × 0.05 × 0.05	0.2 × 0.1 × 0.1	0.2 × 0.1 × 0.1
θ range for data collection [°]	2.03–29.97	2.63–30.00	2.07–29.96
Index ranges	$-15 \le h \le 15$ $-20 \le k \le 20$ $0 \le l \le 32$	$-16 \le h \le 17$ $-17 \le k \le 17$ $0 \le l \le 18$	$-17 \le h \le 17$ $-18 \le k \le 16$ $0 \le l \le 20$
Reflections collected/unique	20429/20492 [R_{int} = 0.0180]	12217/8202 [R_{int} = 0.0609]	11474/11474 [R_{int} = 0.0000]
Refinement method	full-matrix least-squares on F^2	full-matrix least-squares on F^2	full-matrix least-squares on F^2
Data/restraints/parameters	20429/0/851	8202/0/416	11474/6/379
Goodness-of-fit on F^2	0.908	1.125	0.859
Final R indices [$I > 2\sigma(I)$]	R_1 = 0.0516, wR_2 = 0.1174	R_1 = 0.0616, wR_2 = 0.1808	R_1 = 0.0484, wR_2 = 0.1091
R indices (all data)	R_1 = 0.1326, wR_2 = 0.1449	R_1 = 0.0862, wR_2 = 0.1978	R_1 = 0.1826, wR_2 = 0.1479
Largest diff. peak and hole [e Å^{-3}]	0.824 and –0.979	0.950 and –0.856	0.947 and –0.824

Table 9. Crystal and structure determination data.

Compound	**6**	**7**·4CH_2Cl_2·2H_2O	**9**·3.5CH_2Cl_2
Empirical formula	$C_{41}H_{34}Au_2N_2P_2$	$C_{42}H_{36}Au_2N_2P_2$	$C_{62}H_{51}Au_3N_3P_3$
Formula weight	1010.58	1400.34	1819.11
Temperature [K]	293(2)	193(2)	193(2)
Wavelength [Å]	0.71073	0.71073	0.71073
Crystal system	triclinic	triclinic	monoclinic
Space group	$P\bar{1}$	$P\bar{1}$	$P2_1/c$
a [Å]	26.381(15)	8.692(5)	14.102(6)
b [Å]	6.845(4)	12.475(5)	14.755(6)
c [Å]	23.218(7)	13.937(5)	33.292(7)
α [°]	90	65.24(2)	90
β [°]	117.64(2)	75.72(3)	100.201(3)
γ [°]	90	71.00(3)	90
V [Å^3]	3714(3)	1286.8(10)	6818(4)
Z	4	1	4
$D_{calcd.}$ [Mg m^{-3}]	1.807	1.807	1.772
Absorption coefficient [mm^1]	8.007	6.210	6.825
F(000)	1928	678	3492
Crystal size [mm]	0.2 × 0.1 × 0.1	0.2 × 0.1 × 0.1	0.2 × 0.1 × 0.1
θ range for data collection [°]	3.11–29.99	1.62–29.99	2.56–30.00
Index ranges	$-33 \le h \le 34$ $-7 \le k \le 8$ $-31 \le l \le 29$	$-10 \le h \le 11$ $-15 \le k \le 17$ $0 \le l < \le 18$	$-19 \le h \le 19$ $0 \le k \le 19$ $0 \le l \le 46$
Reflections collected/unique	12464/4041 [R_{int} = 0.0355]	6173/6173 [R_{int} = 0.0451]	14839/14839 [R_{int} = 0.0438]
Refinement method	full-matrix least-squares on F^2	full-matrix least-squares on F^2	full-matrix least-squares on F^2
Data/restraints/parameters	4041/0/213	6173/9/298	14839/6/749
Goodness-of-fit on F^2	1.135	1.120	1.110
Final R indices [$I > 2\sigma(I)$]	R_1 = 0.0383, wR_2 = 0.1062	R_1 = 0.0425, wR_2 = 0.1269	R_1 = 0.0620, wR_2 = 0.1740
R indices (all data)	R_1 = 0.0413, wR_2 = 0.1087	R_1 = 0.0490, wR_2 = 0.1387	R_1 = 0.0979, wR_2 = 0.1976
Largest diff. peak and hole [e Å^{-3}]	0.826 and –0.701	0.903 and –0.845	0.989 and –0.856

X-ray Crystallography: A prismatic crystal of **4**, **6**, **7** or **9** was selected and mounted on a MAR345 diffractometer with an image plate detector. Reflection data for **3** and **5** were collected with an Enraf–Nonius CAD4 four-cycle diffractometer. The reflections were assumed as observed by applying the condition $I > 2\sigma(I)$. Intensities were collected with graphite monochromated Mo-K_α radiation. Three reflections were measured every 2h as orientation and intensity control, significant intensity decay was not observed. Lorentz polarisation and absorption corrections were made. The structures were solved by direct methods with the use of the SHELXS computer program[66] and refined by full-matrix least-squares method with the SHELX97 computer program[67] (very negative intensities were not assumed). The function minimised was $\Sigma w||F_o|^2-|F_c|^2|^2$, where $w = [\sigma^2(I) + (0.0760P)^2]^{-1}$ (for **3**), $w = [\sigma^2(I) + (0.1217P)^2]^{-1}$ (for **4**), $w = [\sigma^2(I) + (0.0616P)^2 + 7.8257P]^{-1}$ (for **6**), $w = [\sigma^2(I) + (0.0694P)^2 + 1.5419P]^{-1}$ (for **7**), $w = [\sigma^2(I) + (0.1034P)^2]^{-1}$ (for **9**) and $w = [\sigma^2(I) + (0.0718P)^2]^{-1}$ (for **5**); $P = (|F_o|^2 + 2|F_c|^2)/3$, f, f' and f'' were taken from International Tables of X-ray Crystallography.[68] The Final R values as well as further details concerning the resolution and refinement of the all structures are presented in Tables 8 and 9.

CCDC-676516 (for **3**), -676518 (for **4**), -676517 (for **5**), -676519 (for **6**), -676515 (for **7**) and -677298 (for **9**) contain the supplementary crystallographic data for this paper. These data can be obtained free of charge from The Cambridge Crystallographic Data Centre via www.ccdc.cam.ac.uk/data_request/cif.

Supporting Information Available (see footnote on the first page of this article)**:** Solid-state emission spectra of all compounds.

Acknowledgments

Financial support for this work was provided by the Ministerio de Educación y Ciencia (Project CTQ2006–02362/BQU), Acción Integrada Hispano-Portuguesa (HP2006-0101) and Acção Integrada Luso-Espanhola (E-68/07L). L. R. and A. G. thank Fundaçao para Ciência e Tecnologia for a post-doctoral grant (Portugal, SFRH/BPD/26882/2006) and the Universitat de Barcelona for a scholarship, respectively.

[1] M. P. Cifuentes, M. G. Humphrey, *J. Organomet. Chem.* **2004**, *689*, 3968–3981.
[2] J. Vicente, M. T. Chicote, M. D. Abrisqueta, M. C. R. de Arellano, P. G. Jones, M. G. Humphrey, M. P. Cifuentes, M. Samoc, B. Luther-Davies, *Organometallics* **2000**, *19*, 2968–2974.
[3] S. K. Hurst, M. P. Cifuentes, A. M. McDonagh, M. G. Humphrey, M. Samoc, B. Luther-Davies, I. Asselberghs, A. Persoons, *J. Organomet. Chem.* **2002**, *642*, 259–267.
[4] M. Ferrer, M. Mounir, L. Rodriguez, O. Rossell, S. Coco, P. Gomez-Sal, A. Martin, *J. Organomet. Chem.* **2005**, *690*, 2200–2208.
[5] P. Espinet, *Gold Bull.* **1999**, *32*, 127–134.
[6] V. W. W. Yam, K. M. C. Wong, *Top. Curr. Chem.* **2005**, *257*, 1–32.
[7] A. Vogler, H. Kunkely, *Coord. Chem. Rev.* **2001**, *219*, 489–507.
[8] V. W. W. Yam, K. K. W. Lo, *Chem. Soc. Rev.* **1999**, *28*, 323–334.
[9] S. K. Yip, W. H. Lam, N. Y. Zhu, V. W. W. Yam, *Inorg. Chim. Acta* **2006**, *359*, 3639–3648.

[10] M. I. Bruce, M. Jevric, B. W. Skelton, M. E. Smith, A. H. White, N. N. Zaitseva, *J. Organomet. Chem.* **2006**, *691*, 361–370.
[11] M. C. Lagunas, C. M. Fierro, A. Pintado-Alba, H. de la Riva, S. Betanzos-Lara, *Gold Bull.* **2007**, *40*, 135–141.
[12] P. Li, B. Ahrens, A. D. Bond, J. E. Davies, O. F. Koentjoro, P. R. Raithby, S. J. Teat, *Dalton Trans.* **2008**, 1635–1643.
[13] R. J. Puddephatt, *Coord. Chem. Rev.* **2001**, *216*, 313–332.
[14] T. J. Burchell, M. C. Jennings, R. J. Puddephatt, *Inorg. Chim. Acta* **2006**, *359*, 2812–2818.
[15] W. J. Hunks, J. Lapierre, H. A. Jenkins, R. J. Puddephatt, *J. Chem. Soc. Dalton Trans.* **2002**, 2885–2889.
[16] J. Vicente, M. T. Chicote, M. M. Alvarez-Falcon, D. Bautista, *Organometallics* **2004**, *23*, 5707–5712.
[17] J. Vicente, M. T. Chicote, M. M. Alvarez-Falcon, P. G. Jones, *Organometallics* **2005**, *24*, 5956–5963.
[18] N. C. Habermehl, M. C. Jennings, C. P. McArdle, F. Mohr, R. J. Puddephatt, *Organometallics* **2005**, *24*, 5004–5014.
[19] N. C. Habermehl, F. Mohr, D. J. Eisler, M. C. Jennings, R. J. Puddephatt, *Can. J. Chem.* **2006**, *84*, 111–123.
[20] H. S. Tang, N. Y. Zhu, V. W. W. Yam, *Organometallics* **2007**, *26*, 22–25.
[21] C. P. McArdle, M. J. Irwin, M. C. Jennings, J. J. Vittal, R. J. Puddephatt, *Chem. Eur. J.* **2002**, *8*, 723–734.
[22] C. P. McArdle, S. Van, M. C. Jennings, R. J. Puddephatt, *J. Am. Chem. Soc.* **2002**, *124*, 3959–3965.
[23] F. Mohr, D. J. Eisler, C. P. McArdle, K. Atieh, M. C. Jennings, R. J. Puddephatt, *J. Organomet. Chem.* **2003**, *670*, 27–36.
[24] N. C. Habermehl, D. J. Eisler, C. W. Kirby, N. L. S. Yue, R. J. Puddephatt, *Organometallics* **2006**, *25*, 2921–2928.
[25] K. L. Cheung, S. K. Yip, V. W. W. Yam, *J. Organomet. Chem.* **2004**, *689*, 4451–4462.
[26] H. Y. Chao, W. Lu, Y. Q. Li, M. C. W. Chan, C. M. Che, K. K. Cheung, N. Y. Zhu, *J. Am. Chem. Soc.* **2002**, *124*, 14696–14706.
[27] M. Ferrer, L. Rodriguez, O. Rossell, F. Pina, J. C. Lima, M. F. Bardia, X. Solans, *J. Organomet. Chem.* **2003**, *678*, 82–89.
[28] G. E. Coates, C. Parkin, *J. Chem. Soc.* **1962**, 3220–3226.
[29] E. C. Constable, C. E. Housecroft, M. Neuburger, S. Schaffner, E. J. Shardlow, *Dalton Trans.* **2007**, 2631–2633.
[30] A. Pintado-Alba, H. de la Riva, M. Nieuwhuyzen, D. Bautista, P. R. Raithby, H. A. Sparkes, S. J. Teat, J. M. Lopez-de-Luzuriaga, M. C. Lagunas, *Dalton Trans.* **2004**, 3459–3467.
[31] C. M. Che, H. K. Yip, W. C. Lo, S. M. Peng, *Polyhedron* **1994**, *13*, 887–890.
[32] A. Pons, O. Rossell, M. Seco, X. Solans, M. FontBardia, *J. Organomet. Chem.* **1996**, *514*, 177–182.
[33] V. W. W. Yam, *J. Photochem. Photobiol. A* **1997**, *106*, 75–84.
[34] A. Maspero, I. Kani, A. A. Mohamed, M. A. Omary, R. J. Staples, J. P. Fackler, *Inorg. Chem.* **2003**, *42*, 5311–5319.
[35] X. Hong, K. K. Cheung, C. X. Guo, C. M. Che, *J. Chem. Soc. Dalton Trans.* **1994**, 1867–1871.
[36] P. G. Jones, C. Thone, *Acta Crystallogr. Sect. C* **1992**, *48*, 1312–1314.
[37] N. C. Payne, R. Ramachandran, R. J. Puddephatt, *Can. J. Chem.* **1995**, *73*, 6–11.
[38] D. S. Eggleston, D. F. Chodosh, G. R. Girard, D. T. Hill, *Inorg. Chim. Acta* **1985**, *108*, 221–226.
[39] A. L. Balch, E. Y. Fung, M. M. Olmstead, *J. Am. Chem. Soc.* **1990**, *112*, 5181–5186.
[40] D. Li, X. Hong, C. M. Che, W. C. Lo, S. M. Peng, *J. Chem. Soc. Dalton Trans.* **1993**, 2929–2932.
[41] M. C. Brandys, R. J. Puddephatt, *Chem. Commun.* **2001**, 1280–1281.
[42] T. L. Stott, M. O. Wolf, B. O. Patrick, *Inorg. Chem.* **2005**, *44*, 620–627.
[43] S. Onaka, M. Yaguchi, R. Yamauchi, T. Ozeki, M. Ito, T. Sunahara, Y. Sugiura, M. Shiotsuka, M. Horibe, K. Okazaki, A. Iida, H. Chiba, K. Inoue, H. Imai, K. Sako, *J. Organomet. Chem.* **2005**, *690*, 57–68.
[44] S. C. F. Kui, J. S. Huang, R. W. Y. Sun, N. Y. Zhu, C. M. Che, *Angew. Chem. Int. Ed.* **2006**, *45*, 4663–4666.
[45] R. Narayanaswamy, M. A. Young, E. Parkhurst, M. Ouellette, M. E. Kerr, D. M. Ho, R. C. Elder, A. E. Bruce, M. R. M. Bruce, *Inorg. Chem.* **1993**, *32*, 2506–2517.
[46] M. C. Brandys, M. C. Jennings, R. J. Puddephatt, *J. Chem. Soc. Dalton Trans.* **2000**, 4601–4606.
[47] B. C. Tzeng, A. Schier, H. Schmidbaur, *Inorg. Chem.* **1999**, *38*, 3978–3984.
[48] U. E. I. Horvath, S. Cronje, J. M. McKenzie, L. J. Barbour, H. G. Raubenheimer, *Z. Naturforsch., B: Chem. Sci.* **2004**, *59*, 1605–1617.
[49] L. L. Marques, G. Manzoni de Oliveira, E. Schulz Lang, R. A. Burrow, *Z. Naturforsch., B: Chem. Sci.* **2005**, *60*, 318–321.
[50] S. Y. Ho, E. C. C. Cheng, E. R. T. Tiekink, V. W. W. Yam, *Inorg. Chem.* **2006**, *45*, 8165–8174.
[51] P. M. VanCalcar, M. M. Olmstead, A. L. Balch, *Inorg. Chem.* **1997**, *36*, 5231–5238.
[52] M. K. Cooper, K. Henrick, M. Mcpartlin, J. L. Latten, *Inorg. Chim. Acta* **1982**, *65*, L185–L186.
[53] P. Sevillano, M. E. Garcia, A. Habtemariam, S. Parsons, P. J. Sadler, *Met.-Based Drugs* **1999**, *6*, 211–221.
[54] H. L. Milton, M. V. Wheatley, A. M. Z. Slawin, J. D. Woollins, *Polyhedron* **2004**, *23*, 3211–3220.
[55] S. Friedrichs, P. G. Jones, *Acta Crystallogr. Sect. C* **2000**, *56*, 56–57.
[56] V. W. W. Yam, K. K. W. Lo, K. M. C. Wong, *J. Organomet. Chem.* **1999**, *578*, 3–30.
[57] V. W. W. Yam, K. L. Cheung, S. K. Yip, K. K. Cheung, *J. Organomet. Chem.* **2003**, *681*, 196–209.
[58] H. de la Riva, M. Nieuwhuyzen, C. M. Fierro, P. R. Raithby, L. Male, M. C. Lagunas, *Inorg. Chem.* **2006**, *45*, 1418–1420.
[59] R. S. Becker, *Theory and Interpretation of Fluorescence and Phosphorescence*, Wiley-Interscience, New York, **1969**, p. 234–238.
[60] V. W. W. Yam, S. W. K. Choi, K. K. Cheung, *J. Chem. Soc. Dalton Trans.* **1996**, 3411–3415.
[61] V. Pawlowski, H. Kunkely, A. Vogler, *Inorg. Chim. Acta* **2004**, *357*, 1309–1312.
[62] M. Bardaji, P. G. Jones, A. Laguna, M. D. Villacampa, N. Villaverde, *Dalton Trans.* **2003**, 4529–4536.
[63] R. Uson, A. Laguna, *Organomet. Synth.* **1986**, *3*, 322.
[64] L. Dellaciana, A. Haim, *J. Heterocycl. Chem.* **1984**, *21*, 607–608.
[65] W. Hewertson, H. R. Watson, *J. Chem. Soc.* **1962**, 1490–1494.
[66] G. M. Sheldrick, *SHELXL-97*: *A Program for Automatic Solution of Crystal Structure*, University of Göttingen, Göttingen, Germany, **1997**.
[67] G. M. Sheldrick, *SHELXL-97*: *A Program for Crystal Structure Refinement*, University of Göttingen, Göttingen, Germany, **1997**.
[68] *International Tables of X-ray Crystallography*, Kynoch, Birmingham, **1974**, vol. IV, pp. 99–100, 149.

Received: February 13, 2008
Published Online: May 8, 2008

